Embryonic stem cells form an organized, functional cardiac conduction system in vitro

Steven M. White and William C. Claycomb

AJP - Heart 288:670-679, 2005. First published Oct 7, 2004; doi:10.1152/ajpheart.00841.2004

AJP - Heart and Circulatory Physiology publishes original investigations on the physiology of the heart, blood vessels, and lymphatics, including experimental and theoretical studies of cardiovascular function at all levels of organization ranging from the intact animal to the cellular, subcellular, and molecular levels. It is published 12 times a year (monthly) by the American Physiological Society, 9650 Rockville Pike, Bethesda MD 20814-3991. ISSN: 0363-6135, ESSN: 1522-1539. Visit our website at http://www.the-aps.org/.

Am J Physiol Heart Circ Physiol 288: H670–H679, 2005.
First published October 7, 2004; doi:10.1152/ajpheart.00841.2004.

Embryonic stem cells form an organized, functional cardiac conduction system in vitro

Steven M. White and William C. Claycomb

Department of Biochemistry and Molecular Biology, Louisiana State University Health Sciences Center, New Orleans, Louisiana

Submitted 19 August 2004; accepted in final form 5 October 2004

White, Steven M., and William C. Claycomb. Embryonic stem cells form an organized, functional cardiac conduction system in vitro. *Am J Physiol Heart Circ Physiol* 288: H670–H679, 2005. First published October 7, 2004; doi:10.1152/ajpheart.00841.2004.—A functional pacemaking-conduction system is essential for maintaining normal cardiac function. However, no reproducible model system exists for studying the specialized cardiac pacemaking-conduction system in vitro. Although several molecular markers have been shown to delineate components of the cardiac conduction system in vivo, the functional characteristics of the cells expressing these markers remain unknown. The ability to accurately identify cells that function as cardiac pacemaking cells is crucial for being able to study their molecular phenotype. In differentiating murine embryonic stem cells, we demonstrate the development of an organized cardiac pacemaking-conduction system in vitro using the coexpression of the *minK-lacZ* transgene and the chicken GATA6 (cGATA6) enhancer. These markers identify clusters of pacemaking "nodes" that are functionally coupled with adjacent contracting regions. cGATA6-positive cell clusters spontaneously depolarize, emitting calcium signals to surrounding contracting regions. Physically separating cGATA6-positive cells from nearby contracting regions reduces the rate of spontaneous contraction or abolishes them altogether. cGATA6/*minK* copositive cells isolated from embryoid cells display characteristics of specialized pacemaking-conducting cardiac myocytes with regard to morphology, action potential waveform, and expression of a hyperpolarization-activated depolarizing current. Using the cGATA6 enhancer, we have isolated cells that exhibit electrophysiological and genetic properties of cardiac pacemaking myocytes. Using molecular markers, we have generated a novel model system that can be used to study the functional properties of an organized pacemaking-conducting contracting system in vitro. Moreover, we have used a molecular marker to isolate a renewable population of cells that exhibit characteristics of cardiac pacemaking myocytes.

embryoid bodies; pacemaking; electrophysiology; development; cardiac myocyte

SPECIALIZED CELLS of the cardiac pacemaking-conduction system initiate and synchronize atrial and ventricular contractions. Dysfunction of this intricate electrical system in the form of cardiac arrhythmias is a source of significant morbidity and mortality (9). Although several models have been used to study cardiac pacemaking and conducting cells in vitro, the molecular phenotype of these specialized myocytes remains uncharacterized (3, 4, 17, 20, 32, 39). Genetic markers have been shown to delineate components of the cardiac conduction system in vivo; however, the phenotype of cells expressing these markers remains unknown (36). Therefore, an in vitro model system in which differentiating pacemaking cells could be identified and studied as part of a functional tissue or as single cells would be invaluable for examining the molecular and cellular physiology of cardiac pacemaking myocytes.

Although several genetic markers have been used to identify components of the murine cardiac conduction system based on the location of their expression in the heart, it is unclear whether cells expressing these markers actually function as specialized cardiac pacemaking or conducting myocytes (18, 36, 38, 46). Kupershmidt et al. (30) used a gene-targeting approach to replace the coding region of *minK*, which encodes a β-subunit for the cardiac delayed rectifier potassium current (I_K), with *lacZ*. Expression of the *minK-lacZ* transgene has been detected as early as *embryonic day 8.25* in mice and continues to be expressed in adults, where it is confined primarily to the more proximal cardiac conduction system [from the sinoatrial (SA) node through the interventricular bundles] (28, 30). There is additional evidence that *minK* is expressed in the Purkinje cells of the distal conduction system, indicating a more widespread distribution of expression than seen in the *minK* knockout mice (22, 49). Although adult *minK* knockout mice are more prone to atrial arrhythmias than wild-type animals, they exhibit no altered phenotype (30).

Another marker that has been used to identify more discrete components of the specialized cardiac conduction system is the proximal 1.5-kb promoter-enhancer region of the chicken GATA6 gene (cGATA6) (10). Using *lacZ* expression as a reporter of cGATA6 enhancer activity in transgenic mice, Davis et al. (10) demonstrated that cGATA6 is expressed in the cardiac primordia (before expression of *minK* and the formation of the heart tube) (10). Its expression in the adult mouse becomes restricted to regions of the heart that contain the SA and atrioventricular (AV) nodes as well as the AV bundle (bundle of His) (1, 10, 16). Subsequently, Davis et al. (10) created additional lines of transgenic mice in which the cGATA6 enhancer controlled expression of Cre recombinase. These mice were then mated with ROSA26 Cre reporter mice so that clonal populations of cGATA6-positive (*lacZ* positive) cells could be studied developmentally (10). Whereas the cGATA6 enhancer identified the same myocardial regions as the cGATA6-*lacZ* mice, additional discrete populations within the atria and ventricles were also marked (10). However, of all the reported markers of the cardiac conduction system, the cGATA6 enhancer exhibits the earliest and most restricted expression pattern (49).

Embryonic stem (ES) cells differentiated as embryoid bodies (EBs) have been used to develop numerous model systems for

Address for reprint requests and other correspondence: W. C. Claycomb, Dept. of Biochemistry and Molecular Biology, Louisiana State Univ. Health Sciences Center, 1901 Perdido St., New Orleans, LA 70112 (E-mail: wclayc@lsuhsc.edu).

The costs of publication of this article were defrayed in part by the payment of page charges. The article must therefore be hereby marked "*advertisement*" in accordance with 18 U.S.C. Section 1734 solely to indicate this fact.

studying cardiac myocyte differentiation because they closely recapitulate developmental gene expression patterns in vitro (33, 47). When differentiated as clusters termed EBs, ES cells are capable of differentiating into any cell type in the body, including cells that constitute the specialized cardiac pacemaking-conduction system in vivo (33). We have used the cGATA6 and *minK* markers simultaneously in differentiating murine ES cells (EBs) to demonstrate the development of functional, organized cardiac pacemaking and conducting systems in vitro. Because the cGATA6 enhancer identifies cells that organize and function as pacemaking cells, we used this marker to isolate a population of cells that resemble nodal cardiac myocytes with regard to gene expression and electrophysiological properties.

MATERIALS AND METHODS

Culture and genetic modifications of ES cells. Murine J1 ES cells [kindly provided by the laboratory of Jaenisch (31)] were cultured as previously described (32). Briefly, undifferentiated ES cells were cultured in medium containing 10^3 U/ml leukemia inhibitory factor (Chemicon) in 10-cm^2 0.1% gelatin-coated dishes and passaged every 48 h. Undifferentiated ES cells were transfected with linearized *minK-lacZ* targeting vector [kindly provided by Kuperschmidt et al. (30)] using LF2000 (Invitrogen) according to the manufacturer's protocol. Transfected ES cells were cultured for 7 days in the presence 300 μg/ml G418 (AG Scientific) and 20 μM ganciclovir (Sigma). The proximal 1.5-kb (−1.5/0.0) region of the chicken GATA6 promoter/enhancer (cGATA6) [kindly provided by Burch's laboratory (10)] was inserted into the *Sal*1 and *Bam*HI sites in the multiple cloning site of the promoterless enhanced red fluorescent protein (ERFP) vector (Clontech). After a second period of selection in the same concentrations of G418 and ganciclovir, the undifferentiated ES cells containing the *minK-lacZ* targeting vector were cotransfected with the linear cGATA6 −1.5/0.0-kb enhancer (cGATA6)-ERFP vector and the linear pcDNA3.1(+)-hygro vector (Invitrogen) using LF2000 and selected with 300 μg/ml hygromycin (Sigma) for 7 days.

Differentiation of genetically modified ES cells as EBs. Once undifferentiated ES cells containing both vector constructs (*minK-lacZ* and cGATA6-ERFP) were generated, they were differentiated using the "hanging-drop" method as previously described (32). Briefly, 20-μl drops containing 200 ES cells each in differentiation medium (growth medium without leukemia inhibitory factor) were placed on nontreated (tissue culture) petri dishes (Fisher), which were inverted for 2 days. These EBs in hanging drops were then suspended in differentiation medium in the same dishes for an additional 5 days. At *day 7* of differentiation, EBs were plated onto tissue culture dishes coated with 0.1% gelatin where they remained until used for experiments.

Imaging of EBs and single cells. Initially, EBs made from ES cells containing the *minK-lacZ* transgene were fixed and stained for β-galactosidase expression using the Stratagene β-galactosidase staining kit. For visualizing *minK*-positive cells, EBs were incubated the day of recording for 20 min at 37°C in medium containing 20 μM fluorescein digalactoside (FDG-C12) (Molecular Probes). Cells were then washed with phosphate-buffered saline and incubated for 1 h in differentiation medium before visualization. For fluorescence microscopy, cGATA6-positive cells (ERFP) were detected using a rhodamine filter, whereas *minK-lacZ* cells (green) were imaged using the FITC filter. All imaging (fluorescent and phase/contrast) was performed using a Nikon microscope along with MetaMorph Software (version 5.0 v6, Advanced Scientific).

Calcium imaging. For imaging calcium fluorescence, EBs were loaded with 10 μM of the membrane-permeant acetoxymethyl ester derivative of the fluorescent calcium indicator Calcium Green (Molecular Probes) for 30 min at 37°C. The EBs were then washed and incubated for 1 h in differentiation medium before images were acquired. Cells were imaged on a Diaphot TMD (Nikon) inverted microscope using the ×20 objective. Images were captured using a digital camera (Roper Scientific) and analyzed with MetaMorph Software.

Separation of cGATA6-positive cell clusters from spontaneously contracting regions. Spontaneous contractions were counted by direct visualization under the microscope. To separate cGATA6-positive cells from spontaneously contracting regions, a scalpel fixed to a micromanipulator (Eppendorf) was lowered into the EBs between cGATA6-positive and contracting regions and pulled across the EBs. Spontaneous contractions were counted again after the separation.

Isolation and culture of cGATA6-positive cells. To create the selection vector, pcDNA3.1(+)-neo was digested with *Bcl*1 and religated. This resulted in the repositioning of the neomycin resistance gene (*neo*) immediately downstream of the multiple cloning site. The proximal 1.5-kb (−1.5/0.0) region of the cGATA6 (10) was inserted between the *Sal*1 and *Bam*HI sites in the multiple cloning site of the modified pcDNA3.1(+)-neo vector (with the *Bcl*1 fragment removed). In this newly formed vector, *neo* expression is controlled by the cGATA6 promoter. To enrich the population of cells containing the cGATA6-neo vector, linearized cGATA6-neo was cotransfected with linear pcDNA3.1(+)-hygro using LF2000 (Invitrogen). Transfected, undifferentiated ES cells were cultured for 7 days in ES growth medium containing 200 μg/ml hygromycin (AG Scientific) before being used for experiments.

J1 ES cells containing the cGATA6-neo vector were differentiated using a suspension protocol as previously described (27). Briefly, 3×10^6 ES cells were placed into a nontreated (tissue culture) petri dish (Fisher), which contained differentiation medium, and cultured for 3 days. After 3 days in suspension culture, EBs were plated onto tissue culture dishes (10 cm^2) coated with 0.1% gelatin where they continued to develop. On *day 7* of differentiation, EBs were dispersed into single cells by incubating the EBs in trypsin for 5 min followed by mechanical dissociation using a pipette. After 5 min of centrifugation (1,000 rpm), cells were suspended and plated onto 0.1% gelatin-coated dishes containing differentiation medium with 200 μg/ml G418 (Invitrogen). Each subsequent day, cells were washed multiple times with calcium/magnesium-free phosphate-buffered saline, and fresh medium containing 200 μg/ml G418 was added for a total of 7 days. After 7 days of selection, cells were cultured for 4–6 days in medium containing no G418. After this time, cells were passaged (using trypsin) and plated onto 0.1% gelatin-coated 35-mm dishes.

Gene expression analysis. Total RNA was isolated using the Qiagen RNeasy Kit and was reverse transcribed into cDNA using Superscript III (Invitrogen). Real-time PCR was performed with the ABI Prism 7000 System Detection Sequence (SDS) and software (Applied Biosystems) using SYBR Green (Applied Biosystems) as the detector. Primer sequences are provided in the supplemental table (see http://ajpheart.physiology.org/cgi/content/full/00841.2004/DC1). Gene expression data are shown as the cycle threshold (CT, the lower the number, the higher the gene expression).

Electrophysiological recordings and data analysis. On the day before the recording, EBs were dispersed and plated onto glass coverslips coated with 0.1% gelatin. On the following day, coverslips were transferred to a recording chamber mounted on an inverted microscope (Nikon Diaphot TMD) and superfused with extracellular recording solution. All experiments were conducted at room temperature (22–25°C). Whole cell voltage-clamp and current-clamp experiments were carried out using the standard gigaseal patch-clamp method (21). Recording electrodes were fabricated from 1.5-mm thin-walled borosilicate glass (no. 7052, Garner Glass; Cleremont, CA) using a Flaming-Brown microelectrode puller (P-97, Sutter

Instruments; Novato, CA) and heat polished before use. Each of the pipettes had a tip resistance of 2–5 MΩ when filled with internal solution. Recordings were performed using an Axoclamp 2B patch-clamp amplifier (Axon Instruments; Union City, CA). Data were filtered at 2 kHz, and data were acquired using Clampex 8 software (Axon Instruments). Cells were identified as *minK*- or cGATA6-positive using either the FITC or the rhodamine filters, respectively, during fluorescence microscopy. Action potentials were recorded from spontaneously depolarizing cells or were elicited by stimulation with 2.5-ms, 200-pA square-wave currents. Recordings were made ~1 min following establishment of the whole cell configuration. For current-clamp recordings, the extracellular bath solution contained (in mM) 140 NaCl, 5.4 KCl, 1.8 $CaCl_2$, 1 $MgCl_2$, 10 glucose, and 5 HEPES at pH 7.4 (with NaOH). The intracellular pipette solution contained (in mM) 140 KCl, 10 NaCl, 2 $MgCl_2$, and 5 HEPES at pH 7.3 (with KOH).

Voltage-gated calcium currents (I_{Ca}) were elicited in the whole cell configuration by holding cells at −80 mV for 500 ms and then applying 10-mV steps (500 ms) from −80 to +60 mV and returning to the holding potential of −80 mV. When I_{Ca} was recorded, the extracellular solution contained (in mM) 140 tetraethylammonium-chloride (TEA-Cl), 10 $CaCl_2$, 1 $MgCl_2$, 10 glucose, 5 4-aminopyridine, and 10 HEPES at pH 7.4 (with TEA-OH). The intracellular pipette solution contained (in mM) 140 CsCl, 2 $MgCl_2$, 10 EGTA, 5 Mg-ATP, and 10 HEPES at pH 7.3 (with CsOH).

Hyperpolarization-activated currents (I_f) were elicited in the whole cell configuration by holding cells at −40 mV for 50 ms followed by 10-mV steps (2 s) to −130 mV and returned to −40 mV (50 ms) after each step. After the I_f was recorded, cells were superfused with extracellular solution containing 10 mM cesium chloride. When I_f was measured, the extracellular solution was the same as that used for measuring action potentials (current clamp) except for the addition of 2 mM $BaCl_2$ and 0.5 mM 4-aminopyridine. The intracellular pipette solution contained (in mM) 10 NaCl, 130 K-aspartate, 2 Na_2ATP, 0.1 Na_2GTP, 2 $MgCl_2$, 1 EGTA, 10 HEPES, 10 tetraethylammonium chloride, at pH 7.3 (with KOH).

RESULTS

cGATA6- and minK-positive cell clusters form organized pacemaking-contracting units in EBs. Both the *minK-lacZ* transgene and the cGATA6 enhancer mark regions of the cardiac pacemaking and conducting system in vivo. We first examined the expression of the *minK-lacZ* transgene in EBs to determine whether cells expressing this marker were present in a localized or diffuse pattern. Approximately 100 EBs generated from ES cells containing the *minK-lacZ* targeting vector were fixed and stained for β-galactosidase expression on *day 16* of differentiation. All of the EBs stained positively for expression of the *minK-lacZ* transgene. Cells expressing the *minK-lacZ* transgene were present in small clusters within EBs as shown in Fig. 1*A*.

To determine whether the *minK-lacZ* transgene and the cGATA6 enhancer identify the same cells, we generated EBs from ES cells containing both the *minK-lacZ* transgene and ERFP under transcriptional control of the cGATA6 enhancer. By incubating EBs with the fluorescent β-galactosidase substrate FDG, we are able to detect expression of both vectors simultaneously in live cells using fluorescent microscopy. In Fig. 1, *B* and *C*, *minK* expression is represented by green, whereas ERFP expression (red) marks cGATA6-positive cells within EBs. The cGATA6 enhancer is first expressed in these EBs at approximately *day 5* of differentiation, whereas *minK* expression is not detected until *day 8* (when spontaneous contractions are first observed). Although *minK* is expressed in discrete cell clusters, expression of cGATA6 is restricted to a subpopulation of *minK*-positive cells, recapitulating their expression patterns in vivo (10, 30). In fact, cells expressing *minK* extend from cGATA6-positive clusters and merge with nearby spontaneously contracting regions (Fig. 1, *B–D* and supplemental *movie 1*; http://ajpheart.physiology.org/cgi/

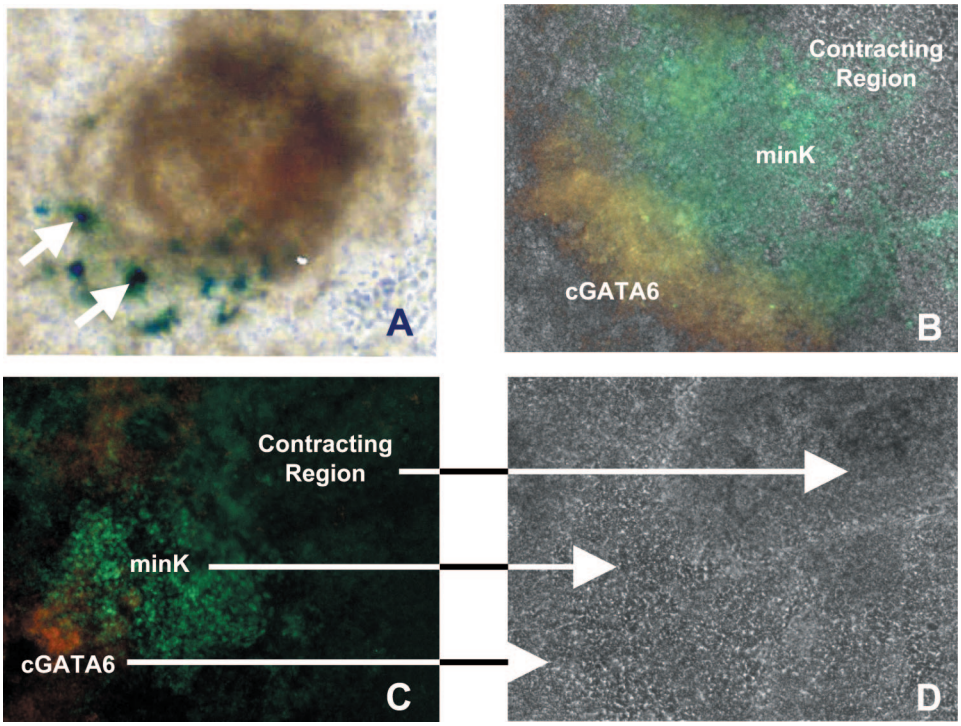

Fig. 1. Coexpression of chicken GATA6 (cGATA6) and *minK* depicts a cardiac conduction system in embryoid bodies (EBs). *A*: staining for β-galactosidase expression reveals distinct clusters of *lacZ*-positive cell clusters in a representative EB generated from embryonic stem (ES) cells expressing the *minK-lacZ* targeting vector. *B*: coexpression of cGATA6 (red) and *min*K (green) are shown overlaid on the corresponding phase-contrast image in a representative EB. *C*: another representative EB region showing a distinct cGATA6-positive "nodal" region (red) with bridging *minK* (green) expression is shown. *D*: phase-contrast image for *C* is shown, which corresponds to supplementary *movie 1* (http://ajpheart.physiology.org/cgi/content/full/00841.2004/DC1), demonstrating the location of the spontaneously contracting region.

content/full/00841.2004/DC1). cGATA6-positive cell clusters are always separated from nearby spontaneously contracting regions. Although there is some heterogeneity with regard to the size and relative location of these cell clusters (as depicted in Fig. 1, *B–C*), the organization with respect to contracting regions is consistent. We examined the expression of *minK* and cGATA6 in more than 30 EBs, which were generated as hanging drops so that the developmental conditions for each EB were as standardized as possible. Approximately 90% of the EBs examined contained spontaneously contracting regions and expressed the *minK-lacZ* transgene and the cGATA6 enhancer in the arrangement depicted in Fig. 1, *B* and *C*. The cellular arrangement depicted by these two molecular markers is strikingly similar to that of the cardiac conduction system in vivo, where a pacemaking node of cells (cGATA6/*minK* copositive) is bridged with working (contracting) myocardium by specialized, rapidly conducting myocytes (*minK* positive).

cGATA6-positive cells clusters initiate rhythmic calcium oscillations. Fluorescent calcium-sensitive dyes are useful for demonstrating functional coupling as well as excitation propagation in vitro (48). To determine whether cGATA6 actually identifies pacemaking or "nodal" structures, EBs were incubated with a calcium-sensitive fluorescent dye (Calcium Green) and imaged before and after the onset of spontaneous contractions. Calcium-dependent depolarizations generated by nodal (pacemaking) myocytes are propagated throughout the heart to control myocardial contractions (43). The cGATA6-positive clusters display a higher basal calcium concentration than surrounding cells. By *day 6* of differentiation, before the onset of visible spontaneous contractions, rhythmic, spontaneous calcium oscillations are observed in cGATA6-positive cell clusters (Fig. 2, *A–C,* and supplemental *movie 2;* http://ajpheart.physiology.org/cgi/content/full/00841.2004/DC1). After the onset of spontaneous contractions (*day 10* of differentiation), calcium oscillations are observed emitting from cGATA6-positive clusters, extending into contractile regions (Fig. 2, *D–F* and supplemental *movie 3*). The rhythmic calcium oscillations emitted from cGATA6-positive cell clusters into nearby contracting regions persists at *days 10* and *20* (last time point measured, data not shown) of differentiation.

cGATA6-positive cell clusters control the rate of contraction in EBs. To determine whether cGATA6-positive clusters are functionally coupled with contracting regions, we performed experiments in which we physically separated the cGATA6-positive cells from nearby contracting regions. After cGATA6-positive cell clusters were identified near spontaneously contracting regions, a scalpel blade attached to a micromanipulator was lowered between the two regions and quickly pulled through the EB so that there was complete separation of the noncontracting, cGATA6-positive region from the nearby spontaneously contracting region without any discernable tissue destruction. In this set of experiments, we found that physical coupling between the two cell populations affects contraction rate (Fig. 3, *A* and *B*). Physically separating these two regions either reduces the spontaneous contraction rate from 56.5 ± 10 to 17 ± 7.5 contractions/min ($n = 11$, $P < 0.01$) or causes cessation of spontaneous contractions (Fig. 3*C*). To control for the effects of tissue destruction within the EBs, cuts were made on the opposite side of spontaneously contracting regions, away from the cGATA6 clusters. None of the control cuts caused a change in contraction rate.

cGATA6-minK copositive cells display characteristics of cardiac pacemaking myocytes. The cell clusters that function as pacemaking nodes in this model system express both the

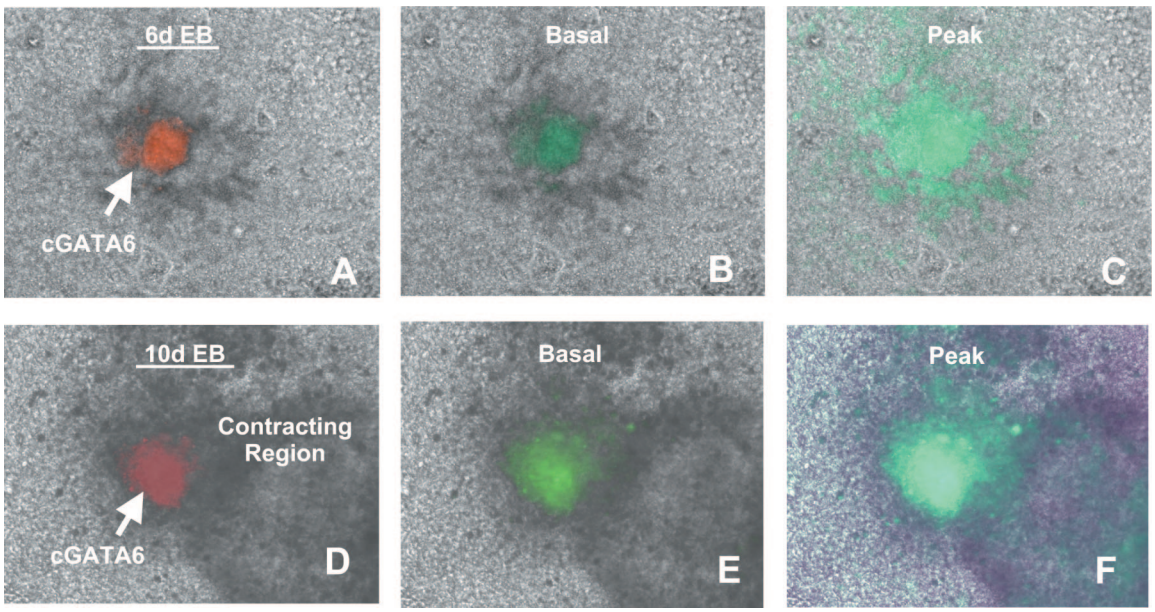

Fig. 2. Calcium sparks are emitted from cGATA6-positive cell clusters before the onset of spontaneous contractions. *A*: representative region of an EB (6 days of differentiation, 6d EB) before the onset of visible spontaneous contractions demonstrating the cGATA6-positive cell cluster (red). *B* and *C*: calcium imaging frames from the same EB region (*A*) at rest (*B*) and during depolarization (*C*) are shown overlaid on phase-contrast images of the same region (corresponding with supplementary *movie 2*; http://ajpheart.physiology.org/cgi/content/full/00841.2004/DC1). *D*: same EB 4 days later (10 d EB) demonstrating the cGATA6-positive cells (red). *E* and *F*: calcium imaging frames from the same EB region (*D*) at rest (*E*) and during contraction (*F*) are shown overlain on phase-contrast images of the same region (corresponding with supplementary *movie 3*). Note the calcium oscillations (green) originating from the cGATA6-positive cell clusters (red).

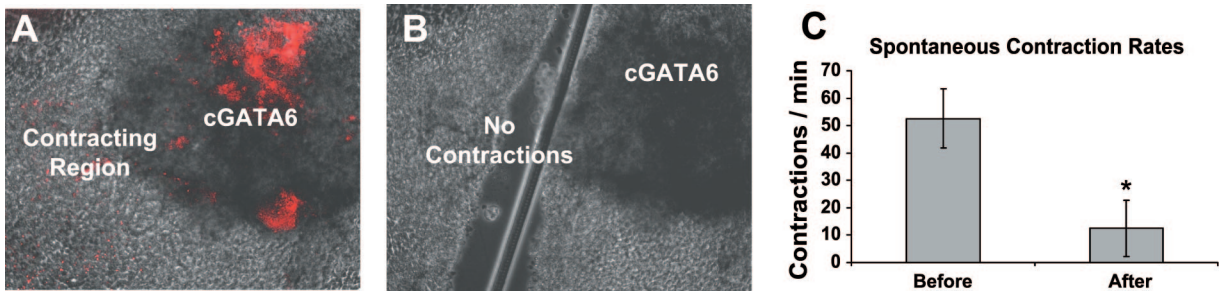

Fig. 3. Separating spontaneously contracting regions from cGATA6-positive cell clusters reduces spontaneous contraction frequency. *A*: representative region of an EB shows the spatial relationship between a cGATA6-positive cell cluster (red) and an adjacent spontaneously contracting region. *B*: an image of the same region (*A*) following physical separation of the cGATA6-positive cluster and the spontaneously contracting region, which resulted in the cessation of contractions. *C*: separating the cGATA6-positive cells from adjacent spontaneously contracting regions caused either a marked reduction or cessation of spontaneous contractions ($*P < 0.05$, $n = 11$).

cGATA6 enhancer as well as the *minK-lacZ*. Therefore, we performed experiments to examine the electrophysiological characteristics of cGATA6-*minK* copositive cells. Spontaneously contracting EBs (differentiation *day 15*) expressing both markers were dissociated into single cells and used for patch-clamp experiments. Isolated cells expressing both cGATA6 and *minK* exhibited two different morphologies. Cells displaying a "nodal" morphology (51) (Fig. 4*A*) exhibit action potential waveforms characteristic of cardiac nodal cells with a prominent diastolic (*phase 4*) depolarization (Fig. 4*C*). Other cGATA6-*minK* cells with morphologies similar to an adult, contracting myocytes (Fig. 4*B*) display atrial-like action poten-

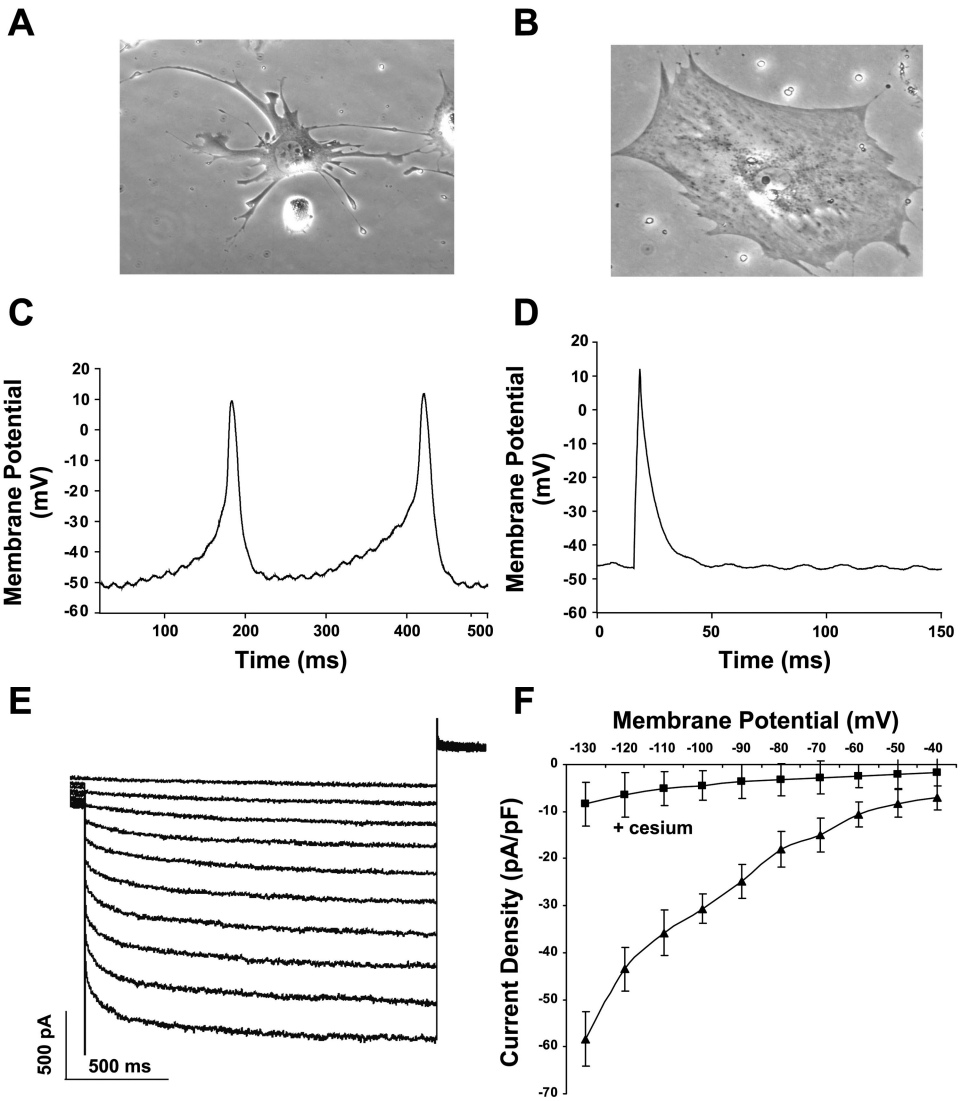

Fig. 4. cGATA6-*minK* copositive cells display characteristics of cardiac pacemaking-conducting cells. *A*: representative cGATA6-*minK* copositive cell corresponds with a typical "nodal" spontaneous action potential associated with that particular morphology (*C*). *B*: another typical morphology observed in cGATA6-*minK* copositive cells is shown with a corresponding "atrial-like" action potential (stimulated) waveform (*D*). *E*: representative traces from a cGATA6-*minK* copositive cell demonstrating the inward hyperpolarization-activated cation current characteristic of nodal cells. *F*: current-voltage relationship for hyperpolarization-activated currents measured in cGATA6-*minK* copositive cells before (triangles) and after (squares) treatment with 10 mM cesium chloride. Points represent mean values at each membrane potential, error bars ± SE; $n = 16$ cells.

tial waveforms (Fig. 4*D*). Approximately 10% of the cGATA6-*minK* copositive cells exhibit nodal characteristics with respect to their morphology and action potential waveform.

An important characteristic of a cardiac pacemaking myocyte is the expression of an inward, hyperpolarization-activated cation current (i.e., I_f). This current was initially termed the "funny" current because it carried an inward, depolarizing current at negative (resting) membrane potentials (13). Although most cardiac myocytes exhibit an I_f, cells in the SA and AV nodes express a much larger I_f current (different current densities and kinetics), which causes them to spontaneously depolarize at a faster rate than other myocytes (11). With the use of the whole cell configuration of the patch-clamp technique, I_f was elicited using hyperpolarizing steps in 10-mV increments from −40 mV to −130 mV from a holding potential of −40 mV. Remarkably, all GATA6-*minK* copositive cells exhibit a large cesium-sensitive I_f (Fig. 4, *E* and *F*). The current (in pA) was normalized to cell size, which is represented by membrane capacitance (in pF). In 16 cells, the maximal I_f density (at a membrane potential of −130 mV) was 58.4 ± 5.7 pA/pF. The reversal potential of this current was at −20 mV (data not shown), and it was significantly inhibited by 10 mM cesium chloride (8.4 ± 4.6 pA/pF, $P < 0.001$). Together, these properties demonstrate that this current is I_f (12).

Isolated cGATA6-positive cells exhibit electrophysiological properties and gene expression profile characteristic of cardiac pacemaking cells. To isolate a pure population of cGATA6-positive cells, we created an ES cell population containing a vector in which expression of the neomycin resistance gene (*neo*) was controlled by the cGATA6 enhancer. This allowed us to select for a population of cells that were resistant to G418 (neomycin), indicating that the cGATA6 enhancer was active. On *day* 7 of differentiation, EBs made from ES cells containing the cGATA6-neo vector were dispersed into single cells and plated onto dishes with medium containing 200 μg/ml G418. Relative to the number of cells before selection, very few cells survived drug selection (Fig. 5*A*). Approximately 10–14 days after the completion of selection, colonies of cells with a similar morphology could be observed (Fig. 5*B*).

Cardiac pacemaking cells exhibit characteristic electrophysiological properties, including expression of I_{Ca} carried primar-

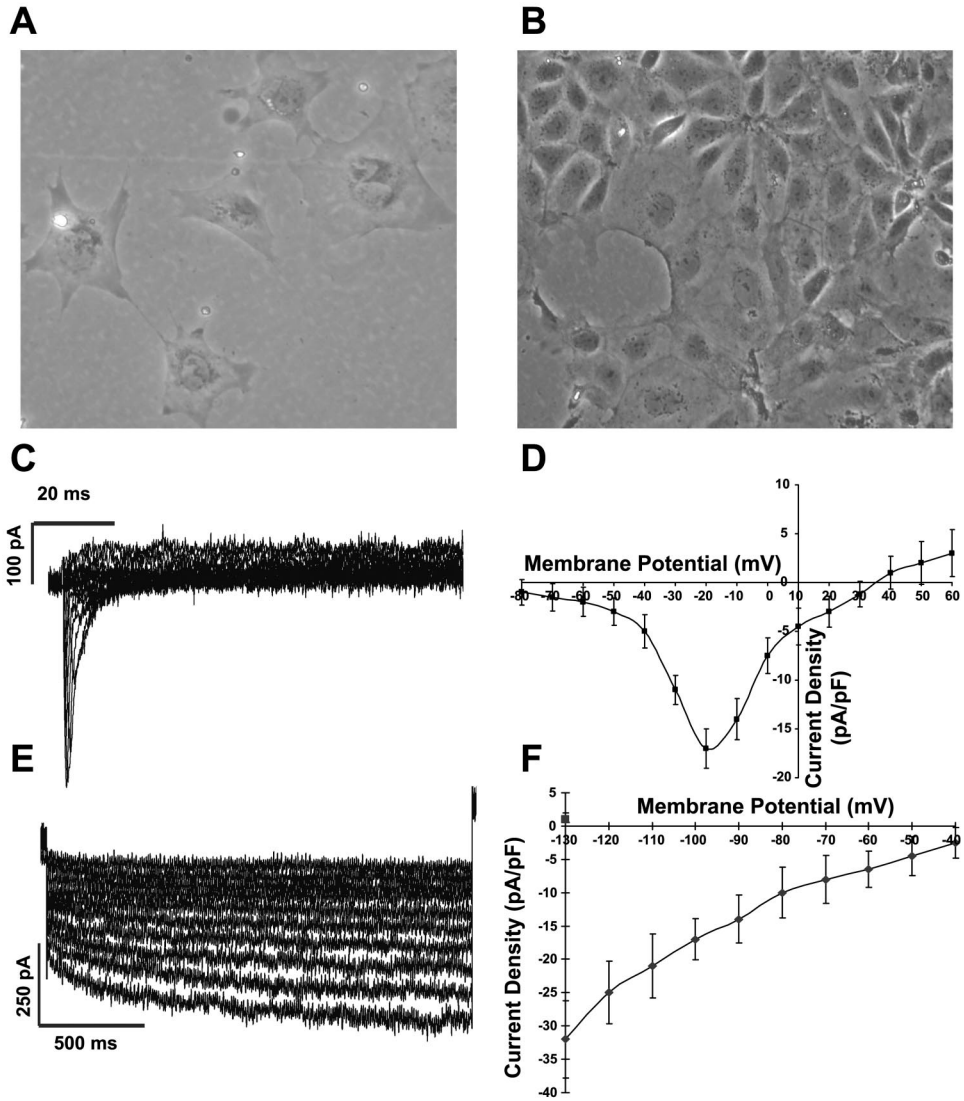

Fig. 5. Isolated cGATA6-neo cells display characteristics of cardiac pacemaking cells. *A*: single cGATA6-neo cells 4 days following the end of G418 selection (*day 16* of differentiation). *B*: approximately 10 days after G418 selection (*day 22* of differentiation), cGATA6-neo cells are seen growing in clusters. *C*: representative traces from a cGATA6-neo cell demonstrating a voltage-gated calcium current (10-mV voltage steps from −80 to +60 mV from a holding potential of −80 mV). *D*: graph of the average current-voltage relationship for the calcium current ($n = 6$ cells). *E*: representative traces from a cGATA6-neo cell demonstrating the inward hyperpolarization-activated cation current. *F*: graph of the average current-voltage relationship ($n = 5$ cells). Points represent mean values at each membrane potential, error bars ± SE.

ily by T-type calcium channels as well as I_f (5). The cGATA6-neo cells express I_{Ca} (Fig. 5*C*) with a current-voltage relationship (Fig. 5*D*), indicating that T-type channels predominate (peak current at −20 mV, $n = 10$ cells) (52). Selected cGATA6-neo cells also express a large I_f (Fig. 5, *E* and *F*) with a current density of 32 ± 5.8 pA/pF ($n = 12$ cells).

Gene expression analysis was performed to better understand the molecular phenotype of these pacemaking cells. Using real-time RT-PCR, we examined the expression of 34 genes (Table 1), which indicate a unique profile of these cells. In addition to expressing characteristic cardiac-specific markers, cGATA6-positive cells also express other genes that indicate these cells represent a primitive cardiac myocyte population. Whereas the selected cells express an anticipated high level of GATA6, they also express significant levels of the cardiac transcription factors *Nkx2.5* and *GATA4* (much more than *MEF2c*). Because cells of the cardiac conduction system are thought to display a partial skeletal muscle transcriptional profile (45), we examined *MyoD*, which is expressed in the cGATA6-neo cells. However, the most highly expressed transcription factor of the ones that we examined is *Msx2* (64-fold higher than *Nkx2.5*), which is expressed in the atrioventicular nodal region in chickens (8). Whereas *Msx2* is involved in many processes such as limb development, it also has a significant role in tissue regeneration (7, 29, 37). The T-box transcription factors *Tbx2* and *Tbx3* are considered markers of primitive cardiac myocytes (35) with *Tbx3* marking regions of the proximal conduction system in the adult heart (24). In the cGATA6-neo cells, *Tbx3* is expressed at a high level (34-fold higher than *Tbx2* and 9-fold higher than *Tbx5*).

Table 1. *Gene expression in cGATA6-neo cells*

Reference	Relative Expression	Cycle Threshold
1. GAPDH		14.9
2. Neo	****	22.2
Transcription factors		
3. GATA4	****	21.8
4. GATA6	****	20.7
5. MEF2C	**	27.7
6. Msx2	*****	18.3
7. MyoD	*	29.2
8. Nkx2.5	***	24.3
9. Tbx2	*	29.2
10. Tbx3	***	24.1
11. Tbx5	**	27.3
Structural proteins		
12. α-Cardiac actin	****	21.0
13. α-Skeletal actin	*****	17.5
14. α-MHC	****	21.7
15. β-MHC	****	24.0
16. MLC-2a	****	21.2
17. MLC-2v		>40
18. Desmin	****	21.1
19. ANF	*	30.5
Ion channels and connexins		
20. Connexin 40	*	28.9
21. Connexin 43	*****	18.7
22. Connexin 45	***	25.4
23. Cav1.2	**	27.4
24. Cav1.3	***	24.4
25. Ryr2	*	28.9
26. Ncx1	**	28.0
27. Scn5a	***	26.0
28. Kir2.1	*	28.7
29. KACh	****	23.3
30. minK	**	27.7
31. HCN-1	*	28.6
32. HCN-2	***	24.1
33. HCN-3	***	24.5
34. HCN-4	*	28.5

Average ($n = 2$ isolations) cycle thresholds are shown (lower numbers indicate a higher level of gene expression). Genes were grouped according to cycle thresholds into the following: ***** < 20; **** 20–24; *** 24–26; ** 26–28; and * > 28. See text for definitions of abbreviations.

cGATA6-neo cells express several cardiac structural and sarcomeric proteins. Of all the genes we examined (except for *GAPDH*), the most highly expressed was α-skeletal actin, which is expressed 12-fold higher than α-cardiac actin. Although β-myosin heavy chain (*β-MHC*) is expressed at a significant level, these cells express fivefold more *α-MHC* than *β-MHC*. With regard to the myosin light chain (MLC) isoforms, the atrial *MLC-2a* isoform is expressed at a high level while expression of the ventricular *MLC-2v* isoform cannot be detected (up to 40 PCR cycles). Additionally, the cGATA6-neo cells express a high level of *desmin*, which is a marker of striated myocytes, and a very low level of atrial natriuretic factor (*ANF*), which is considered to be an early marker of chamber (atrial or ventricular) working myocardium (25).

We examined the expression of 15 genes encoding ion channel subunits and connexins. Of the three connexin isoforms found in cardiac myocytes, cGATA6-neo cells express *connexin 43* 105-fold more than *connexin 45*, which is expressed 11-fold more than *connexin 40*. Expression of the T-type calcium channel subunit gene *Cav1.3* is eightfold higher than the L-type calcium channel subunit *Cav1.2*. cGATA6-neo cells express significant levels of genes encoding the cardiac ryanodine receptor (*Ryr2*), the sodium-calcium exchanger (*NCX1*), the cardiac voltage-gated sodium channel (*Scn5A*), and *minK*. Expression of *Kir3.1*, which encodes the acetylcholine-gated potassium channel (K_{ACh}), is 42-fold higher than the expression of *Kir2.1*, which encodes the inward rectifier potassium channel. With regard to the gene isoforms encoding the hyperpolarization-activated, cyclic nucleotide-gated (*HCN*) channels, which are involved in cardiac pacemaking, the *HCN2* isoform is the most highly expressed. The relative expression of the four isoforms is *HCN 2* ≥ *HCN 3* > *HCN 4* ≥ *HCN 1* (low level of expression).

DISCUSSION

All of the genetic markers of the cardiac conduction system currently available have been designated as such based on the location of their expression. None of the putative markers of the cardiac conduction system have been shown to identify cells that actually function as specialized cardiac pacemaking or conducting cells. Kupershmidt et al. (30) demonstrated that expression of the *minK-lacZ* transgene was colocalized with connexin 40 in cells of the interventricular bundle branches. Several markers have been shown be localized to regions of the specialized cardiac conduction system based on patterns of β-galactosidase staining and action potential propagation (optical mapping) (30, 38). However, no one has isolated single cells expressing any of these markers to determine whether these cells display characteristics of cardiac pacemaking or conducting cells. We have used differentiating ES cells (as EBs) containing two markers of the cardiac conduction system to demonstrate the development of an organized pacemaking-

contracting system in vitro as well as to describe genetic and electrophysiological characteristics of cells identified by these markers.

The murine heart tube forms at approximately *day 8* of embryonic development at which time slow, peristaltic contractions occur. Between 8 and 10 days of differentiation, rhythmic spontaneous contractions can be observed in murine EBs, indicating the presence of cardiac myocytes. In addition to the presence of contracting cardiac myocytes, specialized pacemaking and conducting cells are also present in developing EBs (32). The spontaneously contracting regions observed in differentiating EBs contain cells with electrophysiological characteristics of atrial, ventricular, and pacemaking-conducting myocytes (50). Cells with "nodal-like" action potentials have been found in single-cell dispersions of EBs (32), but there is no way to know before electrophysiological experiments are performed which cells in or near a contracting region might be specialized pacemaking or conducting cells. Whereas the development of electrical activity has been studied in EBs plated using multielectrode arrays, this method provides only field potentials in the regions of the surface electrodes and is not always capable of identifying the specific cells that initiate or conduct the action potentials (3, 20, 26). Although developmental gene expression patterns in EBs mimic the patterns observed in vivo, the number and location of various types of cells within EBs is considered to be random (23, 33). The presence of cardiac myocytes in developing EBs is classically confirmed by observing spontaneous contractions. Several groups have used microdissection to isolate spontaneously contracting regions and demonstrated the presence of cells resembling atrial, ventricular, and nodal myocytes based on their electrophysiological properties (14, 32, 52). However, the organization of these cell types within intact EBs has never been fully appreciated due to a lack of appropriate molecular markers.

Using two markers of the specialized cardiac pacemaking and conducting system simultaneously, we have demonstrated organized pacemaking-conducting-contracting units within EBs. Both the *minK-lacZ* transgene and the cGATA6 enhancer identify components of the proximal (SA node to the interventricular bundles) cardiac conduction system (10, 30). Although their expression patterns in vivo seem to partially overlap, the cGATA6 enhancer appears to identify more discrete populations of cells. In EBs, cGATA6-positive cell clusters could be identified at *day 5* of differentiation, whereas *minK*-positive cells were observed at *day 8*, which is when spontaneous contractions are first observed in the EBs. cGATA6 cells are mostly present in fairly compact clusters, while cells expressing the *minK-lacZ* transgene are more diffuse. Approximately 90% of cGATA6-positive cells are also *minK* positive, and they seem to represent a subpopulation of the *minK*-positive cells.

In EBs, every spontaneously contracting region observed was associated with a cGATA6- and *minK*-positive cell cluster. Approximately 10% of the EBs observed did not contain cGATA6- and *minK*-positive cell clusters. These same EBs also contained no spontaneously contracting regions. Therefore, the colocalization of cGATA6- and *minK*-positive cell clusters is necessary for the development of spontaneous contractions in EBs. The cGATA6-positive cells were always separated from the spontaneously contracting regions by a "bridging" *minK*-positive region, which is similar to nodal organization in vivo with the presence of transitional myocytes (2). Although there is some heterogeneity in the arrangement of the marked cell clusters within the EBs (depicted in Fig. 2, *A–C*), they are always organized so that the cGATA6-positive cluster is connected to a nearby spontaneously contracting region by *minK*-positive cells.

Because the organization of the cells identified by the cGATA6 enhancer and the *minK-lacZ* transgene with respect to contracting regions are reminiscent of primitive cardiac conduction system, we designed experiments to test the functionality of such a system. Nodal cardiac myocytes spontaneously depolarize to generate electrical impulses that are propagated to "working" myocytes causing contractions (18). These spontaneous depolarizations are caused primarily by calcium influx (34). When EBs were incubated with a calcium-sensitive dye to image calcium fluxes, we were able to detect rhythmic, spontaneous calcium oscillations being emitted from cGATA6-positive cell clusters into the surrounding contracting regions. These spontaneous calcium oscillations were first observed in the cGATA6-positive clusters on *day 6* of differentiation, before the onset of spontaneous contractions, and continued after the onset of spontaneous contractions. This indicates that nodal myocytes develop functional pacemaking properties before the onset of visible contractions. The ultimate test for the presence of functional pacemaking cells is to uncouple the pacemaking cells from the contracting cells and observe a change in contraction rate. By demonstrating that the rate of spontaneous contractions in EBs is dependent on physical coupling with cell clusters marked by the cGATA6 enhancer, we have shown that these cells function as pacemaking cells in a multicellular environment.

Knowing that cells identified by the cGATA6 enhancer and the *minK-lacZ* transgene function as specialized pacemaking-conducting cells in vitro, we isolated single cells from the EBs to determine their electrophysiological properties. Based on action potential waveforms, cells can generally be classified as nodal (SA or AV), atrial, distal conducting (His-Purkinje), or ventricular. The differences in the action potential waveform shapes from various cardiac myocytes are due to the relative levels of expression of specific ionic currents (11). One common characteristic of cells of the specialized cardiac pacemaking and conducting system is the relatively high expression of I_f (42). Although cGATA6/*minK* copositive cells are heterogeneous with respect to their action potential waveforms (exhibiting both nodal and atrial), all of these cells express a significant cesium-sensitive I_f.

Although the electrophysiological properties of cardiac pacemaking cells are fairly well established, the molecular phenotype of these cells remains unknown. We selected a population of cells that express the neomycin resistant gene (*neo*) under control of the cGATA6 enhancer to analyze the expression of a panel of cardiac genes encoding transcription factors, structural and sarcomeric proteins, ion channels, and gap junction proteins. Some of the results were expected for nodal, pacemaking cells, whereas others provide novel insight into the regulation of these unique cells. The cGATA6-neo cells express significant levels of *Nkx2.5*, *GATA-4*, *GATA-6*, *α-MHC,* and *β-MHC*, and *desmin*, which confirm their identity as cardiac myocytes (15, 41). These cells express a high level of *MLC-2a* (an atrial-specific myosin light chain isoform) and

no detectable *MLC-2v* (a ventricular-specific isoform). Because the SA and AV nodes are located in the right atrium, the *MLC-2a* expression supports their nodal phenotype.

Of the nine transcription factors analyzed, the two most highly expressed are *Msx2* and *GATA6*. In the chicken heart, expression of *Msx2*, which is found in regenerating tissues, has been found only in portions of the specialized conduction system (7, 8, 29, 37). The fact that *Msx2* is expressed at an extremely high level in the cGATA6-neo cells supports the idea that these are more primitive (less differentiated) myocytes. In *Xenopus*, increased expression of GATA6 delays myocardial development by maintaining cardiac myocytes in a primitive state and preventing the progression into differentiated atrial or ventricular myocytes (6). Another transcription factor expressed at a high level in the cGATA6-neo cells is *Tbx3*. Moorman and Christoffels (19, 25, 35) have shown that *Tbx2* and *Tbx3* bind *Nkx2.5* and repress the transcription of ANF and *connexin 40*, which they consider to be markers of more differentiated (chamber) myocytes. Both ANF and *connexin 40* are expressed at very low levels in cGATA6-neo cells. Importantly, *Tbx3* becomes restricted to the SA and AV nodes and an internodal tract in adult mice, indicating that this transcription factor could also serve as a potential marker to identify cardiac pacemaking myocytes (24).

Although the expression of transcription factors and sarcomeric proteins correlate with what is known about cardiac nodal cells, the expression patterns of some of the membrane proteins is unexpected. Of the gap junction proteins expressed in the heart, *connexin 45* is the isoform most highly expressed in the SA and AV nodes (44). Although *connexin 45* is expressed at a moderate level by the cGATA6-neo cells, *connexin 43* (the most predominant cardiac isoform) is expressed at a much higher level. With regard to the *HCN* channel isoforms, which are responsible for I_f, *HCN-2,* and *HCN-3* are more highly expressed in the cGATA6-neo cells than *HCN-1* and *HCN-4*, which are the predominant nodal isoforms in vivo (40). Although these discrepancies in gene expression patterns between the cGATA6-neo cells and nodal myocytes in vivo can be attributed to the culture conditions as isolated cells, this is the first description of the gene expression profile exhibited by cGATA6-positive myocytes.

In summary, we demonstrate that coexpression of the two molecular markers cGATA6 and *minK* in differentiating ES cells reveal a functional cardiac conduction system in vitro. cGATA6-positive cell clusters act as pacemaking units that functionally couple with nearby contracting regions of EBs. This reproducible EB model system and the pacemaking-conducting cells identified by these markers will be an invaluable tool for studying the fundamental biology of cardiac pacemaking cells, designing targeted pharmaceutical agents, and developing novel cellular and tissue-engineered therapies. By isolating ES cell-derived cardiac myocytes with a pacemaking phenotype, we have generated a reproducible cell model system that can be used to probe the differentiation and molecular regulation of cardiac pacemaking cells.

ACKNOWLEDGMENTS

We thank Drs. Anna Brzezinska and T. Bruce Ferguson for supplying electrophysiological equipment and supplies.

GRANTS

This work was supported by funds from National Heart, Lung, and Blood Institute Grant HL-59879, the Joe W. and Dorothy Brown Foundation, and the Alliance for Cardiovascular Researchers.

REFERENCES

1. **Adamo RF, Guay CL, Edwards AV, Wessels A, and Burch JB.** GATA-6 gene enhancer contains nested regulatory modules for primary myocardium and the embedded nascent atrioventricular conduction system. *Anat Rec* 280A: 1062–1071, 2004.
2. **Anderson RH and Ho SY.** The architecture of the sinus node, the atrioventricular conduction axis, and the internodal atrial myocardium. *J Cardiovasc Electrophysiol* 9: 1233–1248, 1998.
3. **Banach K, Halbach MD, Hu P, Hescheler J, and Egert U.** Development of electrical activity in cardiac myocyte aggregates derived from mouse embryonic stem cells. *Am J Physiol Heart Circ Physiol* 284: H2114–H2123, 2003.
4. **Bond J, Sedmera D, Jourdan J, Zhang Y, Eisenberg CA, Eisenberg LM, and Gourdie RG.** Wnt11 and Wnt7a are up-regulated in association with differentiation of cardiac conduction cells in vitro and in vivo. *Dev Dyn* 227: 536–543, 2003.
5. **Boyett MR, Honjo H, and Kodama I.** The sinoatrial node, a heterogeneous pacemaker structure. *Cardiovasc Res* 47: 658–687, 2000.
6. **Brewer A, Gove C, Davies A, McNulty C, Barrow D, Koutsourakis M, Farzaneh F, Pizzey J, Bomford A, and Patient R.** The human and mouse GATA-6 genes utilize two promoters and two initiation codons. *J Biol Chem* 274: 38004–38016, 1999.
7. **Carlson MR, Bryant SV, and Gardiner DM.** Expression of Msx-2 during development, regeneration, and wound healing in axolotl limbs. *J Exp Zool* 282: 715–723, 1998.
8. **Chan-Thomas PS, Thompson RP, Robert B, Yacoub MH, and Barton PJ.** Expression of homeobox genes Msx-1 (Hox-7) and Msx-2 (Hox-8) during cardiac development in the chick. *Dev Dyn* 197: 203–216, 1993.
9. **Cheng CF, Kuo HC, and Chien KR.** Genetic modifiers of cardiac arrhythmias. *Trends Mol Med* 9: 59–66, 2003.
10. **Davis DL, Edwards AV, Juraszek AL, Phelps A, Wessels A, and Burch JB.** A GATA-6 gene heart-region-specific enhancer provides a novel means to mark and probe a discrete component of the mouse cardiac conduction system. *Mech Dev* 108: 105–119, 2001.
11. **DiFrancesco D.** Cardiac pacemaker: 15 years of "new" interpretation. *Acta Cardiol* 50: 413–427, 1995.
12. **DiFrancesco D.** Cesium and the pacemaker current. *J Cardiovasc Electrophysiol* 6: 1152–1155, 1995.
13. **DiFrancesco D.** The contribution of the "pacemaker" current (if) to generation of spontaneous activity in rabbit sino-atrial node myocytes. *J Physiol* 434: 23–40, 1991.
14. **Doevendans PA, Kubalak SW, An RH, Becker DK, Chien KR, and Kass RS.** Differentiation of cardiomyocytes in floating embryoid bodies is comparable to fetal cardiomyocytes. *J Mol Cell Cardiol* 32: 839–851, 2000.
15. **Doevendans PA and van Bilsen M.** Transcription factors and the cardiac gene programme. *Int J Biochem Cell Biol* 28: 387–403, 1996.
16. **Edwards AV, Davis DL, Juraszek AL, Wessels A, and Burch JB.** Transcriptional regulation in the mouse atrioventricular conduction system. *Novartis Found Symp* 250: 177–189; discussion 189–193, 276–179, 2003.
17. **Gassanov N, Er F, Zagidullin N, and Hoppe UC.** Endothelin induces differentiation of ANP-EGFP expressing embryonic stem cells towards a pacemaker phenotype. *FASEB J* 18: 1710–1712, 2004.
18. **Gourdie RG, Harris BS, Bond J, Justus C, Hewett KW, O'Brien TX, Thompson RP, and Sedmera D.** Development of the cardiac pacemaking and conduction system. *Birth Defects Res Part C Embryo Today* 69: 46–57, 2003.
19. **Habets PE, Moorman AF, Clout DE, van Roon MA, Lingbeek M, van Lohuizen M, Campione M, and Christoffels VM.** Cooperative action of Tbx2 and Nkx2.5 inhibits ANF expression in the atrioventricular canal: implications for cardiac chamber formation. *Genes Dev* 16: 1234–1246, 2002.
20. **Halbach M, Egert U, Hescheler J, and Banach K.** Estimation of action potential changes from field potential recordings in multicellular mouse cardiac myocyte cultures. *Cell Physiol Biochem* 13: 271–284, 2003.

21. **Hamill OP, Marty A, Neher E, Sakmann B, and Sigworth FJ.** Improved patch-clamp techniques for high-resolution current recording from cells and cell-free membrane patches. *Pflügers Arch* 391: 85–100, 1981.
22. **Han W, Bao W, Wang Z, and Nattel S.** Comparison of ion-channel subunit expression in canine cardiac Purkinje fibers and ventricular muscle. *Circ Res* 91: 790–797, 2002.
23. **Hescheler J, Fleischmann BK, Lentini S, Maltsev VA, Rohwedel J, Wobus AM, and Addicks K.** Embryonic stem cells: a model to study structural and functional properties in cardiomyogenesis. *Cardiovasc Res* 36: 149–162, 1997.
24. **Hoogaars WM, Tessari A, Moorman AF, de Boer PA, Hagoort J, Soufan AT, Campione M, and Christoffels VM.** The transcriptional repressor Tbx3 delineates the developing central conduction system of the heart. *Cardiovasc Res* 62: 489–499, 2004.
25. **Houweling AC, Somi S, Van Den Hoff MJ, Moorman AF, and Christoffels VM.** Developmental pattern of ANF gene expression reveals a strict localization of cardiac chamber formation in chicken. *Anat Rec* 266: 93–102, 2002.
26. **Igelmund P, Fleischmann BK, Fischer IR, Soest J, Gryshchenko O, Bohm-Pinger MM, Sauer H, Liu Q, and Hescheler J.** Action potential propagation failures in long-term recordings from embryonic stem cell-derived cardiomyocytes in tissue culture. *Pflügers Arch* 437: 669–679, 1999.
27. **Klug MG, Soonpaa MH, Koh GY, and Field LJ.** Genetically selected cardiomyocytes from differentiating embronic stem cells form stable intracardiac grafts. *J Clin Invest* 98: 216–224, 1996.
28. **Kondo RP, Anderson RH, Kupershmidt S, Roden DM, and Evans SM.** Development of the cardiac conduction system as delineated by minK-lacZ. *J Cardiovasc Electrophysiol* 14: 383–391, 2003.
29. **Kritzik MR, Jones E, Chen Z, Krakowski M, Krahl T, Good A, Wright C, Fox H, and Sarvetnick N.** PDX-1 and Msx-2 expression in the regenerating and developing pancreas. *J Endocrinol* 163: 523–530, 1999.
30. **Kupershmidt S, Yang T, Anderson ME, Wessels A, Niswender KD, Magnuson MA, and Roden DM.** Replacement by homologous recombination of the minK gene with lacZ reveals restriction of minK expression to the mouse cardiac conduction system. *Circ Res* 84: 146–152, 1999.
31. **Li E, Bestor TH, and Jaenisch R.** Targeted mutation of the DNA methyltransferase gene results in embryonic lethality. *Cell* 69: 915–926, 1992.
32. **Maltsev VA, Rohwedel J, Hescheler J, and Wobus AM.** Embryonic stem cells differentiate in vitro into cardiomyocytes representing sinus-nodal, atrial and ventricular cell types. *Mech Dev* 44: 41–50, 1993.
33. **Maltsev VA, Wobus AM, Rohwedel J, Bader M, and Hescheler J.** Cardiomyocytes differentiated in vitro from embryonic stem cells developmentally express cardiac-specific genes and ionic currents. *Circ Res* 75: 233–244, 1994.
34. **Mangoni ME, Couette B, Bourinet E, Platzer J, Reimer D, Striessnig J, and Nargeot J.** Functional role of L-type Cav1.3 Ca^{2+} channels in cardiac pacemaker activity. *Proc Natl Acad Sci USA* 100: 5543–5548, 2003.
35. **Moorman AF and Christoffels VM.** Development of the cardiac conduction system: a matter of chamber development. *Novartis Found Symp* 250: 25–34; discussion 34–43, 276–279, 2003.
36. **Myers DC and Fishman GI.** Molecular and functional maturation of the murine cardiac conduction system. *Trends Cardiovasc Med* 13: 289–295, 2003.
37. **Nechiporuk A and Keating MT.** A proliferation gradient between proximal and msxb-expressing distal blastema directs zebrafish fin regeneration. *Development* 129: 2607–2617, 2002.
38. **Rentschler S, Vaidya DM, Tamaddon H, Degenhardt K, Sassoon D, Morley GE, Jalife J, and Fishman GI.** Visualization and functional characterization of the developing murine cardiac conduction system. *Development* 128: 1785–1792, 2001.
39. **Rentschler S, Zander J, Meyers K, France D, Levine R, Porter G, Rivkees SA, Morley GE, and Fishman GI.** Neuregulin-1 promotes formation of the murine cardiac conduction system. *Proc Natl Acad Sci USA* 99: 10464–10469, 2002.
40. **Robinson RB and Siegelbaum SA.** Hyperpolarization-activated cation currents: from molecules to physiological function. *Annu Rev Physiol* 65: 453–480, 2003.
41. **Sachinidis A, Fleischmann BK, Kolossov E, Wartenberg M, Sauer H, and Hescheler J.** Cardiac specific differentiation of mouse embryonic stem cells. *Cardiovasc Res* 58: 278–291, 2003.
42. **Saint DA.** Pacemaking in the heart: the interplay of ionic currents. *Clin Exp Pharmacol Physiol* 25: 841–846, 1998.
43. **Sauer H, Theben T, Hescheler J, Lindner M, Brandt MC, and Wartenberg M.** Characteristics of calcium sparks in cardiomyocytes derived from embryonic stem cells. *Am J Physiol Heart Circ Physiol* 281: H411–H421, 2001.
44. **Severs NJ, Coppen SR, Dupont E, Yeh HI, Ko YS, and Matsushita T.** Gap junction alterations in human cardiac disease. *Cardiovasc Res* 62: 368–377, 2004.
45. **Takebayashi-Suzuki K, Pauliks LB, Eltsefon Y, and Mikawa T.** Purkinje fibers of the avian heart express a myogenic transcription factor program distinct from cardiac and skeletal muscle. *Dev Biol* 234: 390–401, 2001.
46. **Tamaddon HS, Vaidya D, Simon AM, Paul DL, Jalife J, and Morley GE.** High-resolution optical mapping of the right bundle branch in connexin40 knockout mice reveals slow conduction in the specialized conduction system. *Circ Res* 87: 929–936, 2000.
47. **Van Kempen M, van Ginneken A, de Grijs I, Mutsaers N, Opthof T, Jongsma H, and van der Heyden M.** Expression of the electrophysiological system during murine embryonic stem cell cardiac differentiation. *Cell Physiol Biochem* 13: 263–270, 2003.
48. **Viatchenko-Karpinski S, Fleischmann BK, Liu Q, Sauer H, Gryshchenko O, Ji GJ, and Hescheler J.** Intracellular Ca^{2+} oscillations drive spontaneous contractions in cardiomyocytes during early development. *Proc Natl Acad Sci USA* 96: 8259–8264, 1999.
49. **Wessels A, Phelps A, Trusk TC, Davis DL, Edwards AV, Burch JB, and Juraszek AL.** Mouse models for cardiac conduction system development. *Novartis Found Symp* 250: 44–59; discussion 59–67, 276–279, 2003.
50. **Wobus AM, Rohwedel J, Maltsev V, and Hescheler J.** Development of cardiomyocytes expressing cardiac-specific genes, action potentials, and ionic channels during embryonic stem cell-derived cardiogenesis. *Ann NY Acad Sci* 752: 460–469, 1995.
51. **Wu J, Schuessler RB, Rodefeld MD, Saffitz JE, and Boineau JP.** Morphological and membrane characteristics of spider and spindle cells isolated from rabbit sinus node. *Am J Physiol Heart Circ Physiol* 280: H1232–H1240, 2001.
52. **Zhang YM, Shang L, Hartzell C, Narlow M, Cribbs L, and Dudley SC Jr.** Characterization and regulation of T-type Ca2+ channels in embryonic stem cell-derived cardiomyocytes. *Am J Physiol Heart Circ Physiol* 285: H2770–H2779, 2003.